LETTER

doi:10.1038/nature11022

Earth-like sand fluxes on Mars

N. N. Bridges[1], F. Ayoub[2], J-P. Avouac[2], S. Leprince[2], A. Lucas[2] & S. Mattson[3]

Strong and sustained winds on Mars have been considered rare, on the basis of surface meteorology measurements and global circulation models[1,2], raising the question of whether the abundant dunes and evidence for wind erosion seen on the planet are a current process. Recent studies[3–6] showed sand activity, but could not determine whether entire dunes were moving—implying large sand fluxes—or whether more localized and surficial changes had occurred. Here we present measurements of the migration rate of sand ripples and dune lee fronts at the Nili Patera dune field. We show that the dunes are near steady state, with their entire volumes composed of mobile sand. The dunes have unexpectedly high sand fluxes, similar, for example, to those in Victoria Valley, Antarctica, implying that rates of landscape modification on Mars and Earth are similar.

The Martian surface displays abundant bedforms (ripples and dunes)[7], and evidence for wind erosion ranging from centimetre-scale ventifact rock textures[8] to kilometre-scale yardangs and exhumed mantles[7]. But whether these features are actively moving has been an open question, as sand-transporting winds have been considered rare in the low-density atmosphere of Mars[1,2]. Although many bedforms have been interpreted as static, relict features[7], and dune formation times are predicted to be five orders of magnitude slower than on Earth[9], recent high-resolution orbiter[3–6] and rover[10] images have provided evidence of sand movement. Whether these observations document surficial migration, or bedforms in equilibrium (the full volume undergoing movement)— and therefore large sand fluxes capable of actively eroding the surface—could not be determined using the traditional measurement techniques of the earlier studies. Resolution of this problem has implications for understanding past Martian climates, as it has been suggested that significant erosion on Mars may have required a higher-pressure atmosphere in the past[11].

Recent advances in optical image correlation[12] have allowed dune migration rates and associated sand fluxes in terrestrial dune fields to be estimated from satellite data[13]. We took advantage of the High Resolution Imaging Science Experiment (HiRISE) on the Mars Reconnaissance Orbiter, a push-broom imager with pixel sizes of $\sim$25 cm[14], to track the displacement of sand ripples covering the dunes. We implemented the HiRISE geometry in the "Co-registration of Optically Sensed Images and Correlation" (COSI-Corr) tool suite, which provides quantitative surface dynamics measurements by automatic and precise orthorectification, co-registration, and subpixel correlation of images[12]. The resulting data rival those obtained using remotely sensed images of Earth dunes[13].

The high spatial resolution of HiRISE combined with COSI-Corr allows us to quantify dune ripple migration rates and the derivation of sand flux across the entire image, a critical measurement that we perform for the first time on a planetary surface. To undertake this investigation, we chose the Nili Patera dune field, a location containing abundant barchan dunes with morphology typical of dunes elsewhere on Mars and on Earth, and for which localized ripple migration has been identified using visual comparison of images acquired at different times[3,6] (Supplementary Fig. 1). Four HiRISE images centred on the Nili Patera dune field (8.8° N, 67.3° E) were used: two to quantify changes that occurred in the time interval (105 Earth days) between their acquisition (subsequently referred to as images T1 and T2); and another two to construct a stereo-derived Digital Elevation Model, on which the images were orthorectified and co-registered (images S1 and S2; Supplementary Table 1). The correlation of T1 and T2 provides dense measurements of ripple migration (Fig. 1a). We find that ripple migration occurs across the entire dune field, and increases with elevation along the stoss slopes. Measurable ripple motion is up to 4.5 m, confirming high sand activity. As dunes become more sheltered towards the southwest, ripple displacement generally decreases, consistent with active, northeasterly winds. The azimuthal distribution of displacement vectors (Fig. 1a, inset) is consistent with the southwesterly trend inferred from the orientation of the dune slip faces and barchan horns.

Ripple displacement (d_r) increases linearly with elevation on a given dune (h_D) (Fig. 2). The fastest ripples, those with the steepest slopes in Fig. 2, moved so far that the correlation breaks down once the displacement exceeds a distance approximately equal to the ripple wavelength (4.6 ± 0.09 m; see Supplementary Information). This linear relationship is consistent with the behaviour of steady-state migrating dunes in which mass is conserved while shape and volume are maintained[15], and wind shear stress increases with dune elevation[9,16] (see Supplementary Information).

We also measured dune migration from the advancement of lee fronts between T2 and S1 (941 days), taking advantage of the accurate registration of the two images obtained with COSI-Corr. Fronts showed measurable advancement (Supplementary Animation), but were negligible between T1 and T2 (105 d) except for a few isolated cases where avalanches occurred[3,6]. These measurements were performed only where the lee advance was clear, and therefore may not represent the average migration of the whole dune field.

Our measurements of ripples and dune migration are related, as they both reflect sand transport, and can be used to estimate sand flux. Sand transport results from saltation and reptation[17,18]. Saltation is the hopping motion of grains over long trajectories which, when they collide with a sand bed, results in a splash of shorter reptation trajectories. Reptation causes ripple migration, whereas both processes contribute to dune advancement. The reptation sand flux is estimated by multiplying the ripples' migration rate by their average height, h_r, estimated to be 20 ± 6 cm (Supplementary Information). Assuming the reptation sand flux equals that of the whole dune, the dune migration rate is $d_r h_r/(h_D t)$ (Supplementary Information), where t is the time interval (105 d). The histogram of dune migration rates over the whole study area peaks at an average value of $\sim$0.1 m yr^{-1} (Earth year) (Fig. 3). This distribution is consistent with the dune speeds derived from linear fits to the selected ripple profiles of Fig. 2, which range from 0.03 ± 0.01 to 0.27 ± 0.08 m yr^{-1} (Fig. 3). The relative uncertainty in dune migration rate derived from these measurements is estimated to be less than 20% (Fig. 3, inset table); however, this is a minimum estimate because the saltation sand flux contribution is not yet considered. Extrapolating the dune migration rates derived from lee-front advancement to a year shows that the lee-derived rates are approximately five times larger than the ripple-derived rates (Fig. 3).

[1]Space Department, Johns Hopkins University Applied Physics Laboratory, Laurel, Maryland 20723, USA. [2]Division of Geological and Planetary Sciences, California Institute of Technology, Pasadena, California 91125, USA. [3]Lunar and Planetary Laboratory, University of Arizona, Tucson, Arizona 85721, USA.

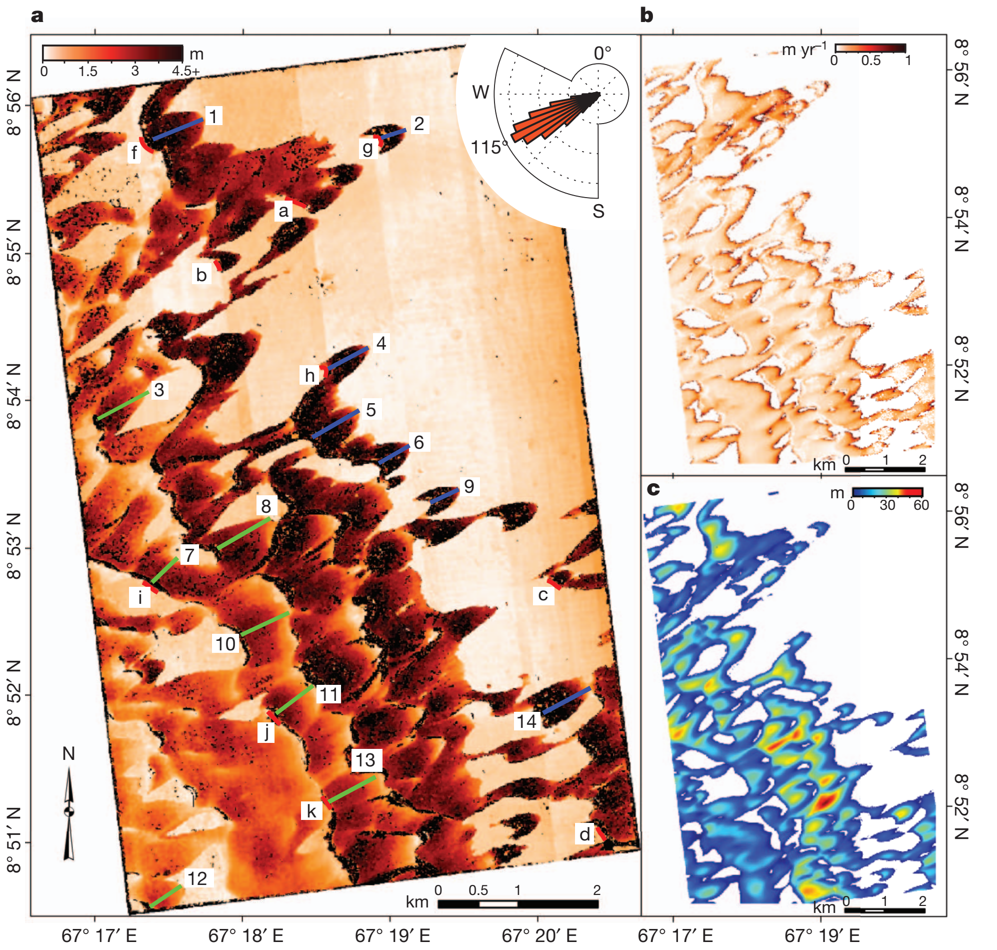

Figure 1 | Ripple migration, dune migration and dune elevation. **a**, Ripple displacements in the Nili Patera dune field derived from correlating HiRISE images PSP_004339_1890 (30 June 2007) and PSP_005684_1890 (13 October 2007). Green and blue numbered lines show where profiles of ripple displacement were retrieved. Red lines with letters show where dune lee-front displacements were measured between images PSP_004339_1890 and ESP_017762_1890 (11 May 2010). Inset rose diagram shows distribution of ripple migration azimuth. **b**, Dune migration rate derived from the ripple migration rates and dune elevation. **c**, Dune elevation relative to bedrock base. Elevation and height maps are based on stereo images ESP_017762_1890 and ESP_018039_1890 (2 June 2010). See Supplementary Information for details of how dune height was estimated.

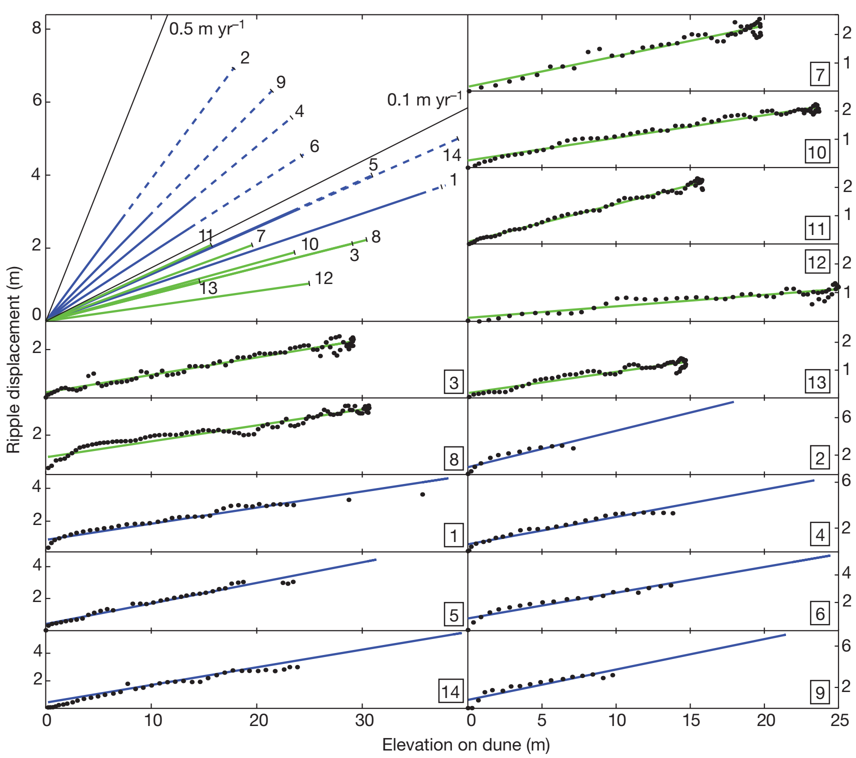

Figure 2 | Linear correlation between ripple migration and dune height. Upper left frame: ripple displacement versus local dune elevation for profiles on upwind (blue) and downwind (green) dunes. Profile locations are shown in Fig. 1a. ('Upwind' dunes are in the northeast part of the field, unsheltered from prevailing northeasterly winds; 'downwind' dunes are in the southwest part of the field, partially sheltered by the dunes to the northeast.) Solid lines are best-fitting linear functions, shifted to go through the origin to facilitate slope comparisons. Dashed lines are extrapolations out to the dune crest for cases where displacements could not be estimated, owing to decorrelation of the ripple patterns. Black lines are isopleths of dune migration rates. The individual profiles and measured ripple displacements are shown in the other frames.

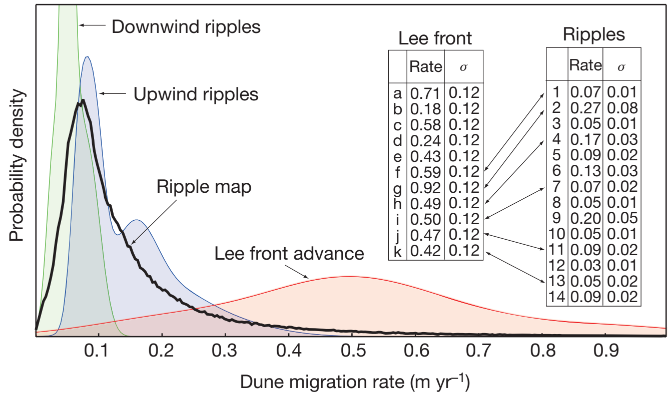

Figure 3 | Dune migration rates. Normalized histogram (black) of dune migration rates over the 105-day T1–T2 time interval, derived from all measurements of Fig. 1b where dune height (elevation above the bedrock base) exceeds 0.5 m. (All time intervals and rates in this paper refer to Earth days and years.) The right-side tail is mostly attributable to rates measured on the dunes' upwind and lateral edges, where the measured rates are probably erroneously large because the ripples there are not fully developed to the equilibrium height that is assumed in the calculations. (See Supplementary Information.) These large values appear as rims around the dunes in Fig. 1b. The blue and green probability density functions show, respectively, the migration rates inferred for individual upwind and downwind dunes (Fig. 2). (See inset tables and Supplementary Table 2 for all migration rates and uncertainties.) The mean heights of the upwind and downwind dunes are 27 and 22 m, respectively. The red probability density function shows migration rates derived from lee-front advance over the 941-day T2–S1 interval. The location of these lee fronts is shown in Fig. 1a (except for measurement e, which is located outside the area shown in the figure). Black arrows between the inset tables link dune migration rates obtained on the same dune from lee-front tracking (thus resulting from reptation and saltation) and from ripple migration (resulting from reptation only). Assumptions about ripple geometry result in uncertainty in the mean height of the ripples (see Supplementary Information), which propagates to a 20% uncertainty in dune migration rate.

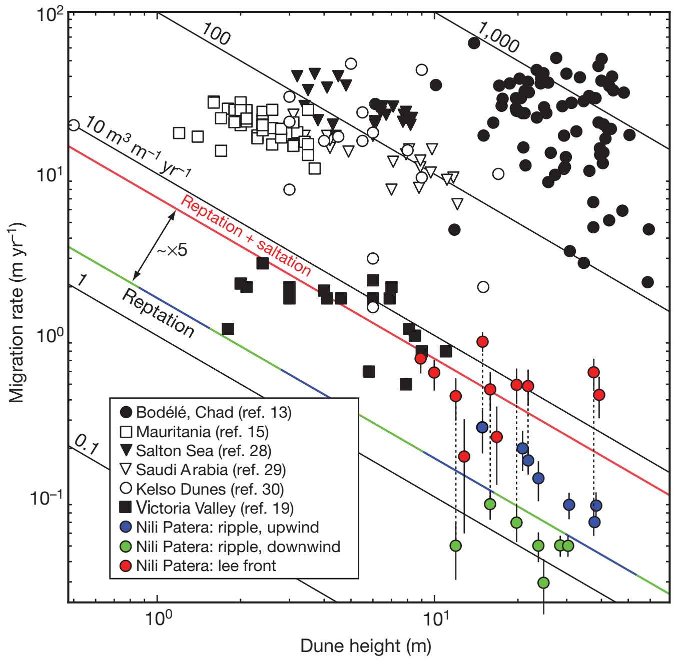

Figure 4 | Comparison of dune migration rates and sand flux on Mars and Earth. Dune migration rates versus dune height for a number of sites on Earth (with reference numbers in parentheses); the 14 dunes selected in Fig. 2; and dunes for which the lee-front advance was measured (locations in Fig. 1a). Black diagonal lines are isopleths of sand flux. Red and blue/green diagonal lines are mean sand fluxes derived from the lee-front advance and ripple migration measurements, respectively. Vertical error bars show 1σ (1 standard deviation) confidence intervals for the dune migration rates. The mean sand flux derived from the lee-front advance is 6.9 ± 0.52 (1σ) $\mathrm{m^3\,m^{-1}\,yr^{-1}}$, and the mean sand flux derived from the ripple migration measurements is 1.4 ± 0.08 $\mathrm{m^3\,m^{-1}\,yr^{-1}}$. (See Supplementary Table 2 for individual measurements.) The factor of five between the two fluxes suggests that the saltation flux is about four times the reptation flux.

The higher values reflect the contribution of the saltation sand flux, which is not considered in the ripple-derived rates.

Comparison with terrestrial dunes (Fig. 4), shows that the Nili migration rates are about 1–2 orders of magnitude slower than for dunes of comparable height on Earth. Multiplying the dune migration rates by their maximum heights (h_{Dmax}) gives sand fluxes at the dune crests: $Q_0 = d_{\mathrm{D}} h_{\mathrm{Dmax}}/t$, where d_{D} is dune displacement[13]. Mean fluxes for reptation and reptation plus saltation are 1.4 and 6.9 $\mathrm{m^3\,m^{-1}\,yr^{-1}}$, respectively (Fig. 4). This is comparable to sand fluxes for dunes in Victoria Valley, Antarctica[19]. Terrestrial studies show that bulk and interdune sand fluxes are about one-third of the crest flux[15], so that typical fluxes in Nili should be $\sim$2.3 $\mathrm{m^3\,m^{-1}\,yr^{-1}}$. The Nili dunes have $\sim$1,000 times the volume of those in Victoria Valley, yet similar sand fluxes, indicating that the characteristic timescales of formation are $\sim$1,000 times longer, showing that dunes on Mars evolve much more slowly than their counterparts on Earth. The timescale associated with the formation and evolution of the Nili Patera dune field, estimated by dividing the dunes' volume by the average sand flux times the length scale of the dune field, is $\sim$9,800 yr. Similarly, turnover times needed for dunes to migrate over a distance equal to their length are very short, ranging from $\sim$170 yr for the fastest dune (Fig. 1a, dune c) to a few thousand years for the slower ones.

The observed correlation between ripple and dune displacement implies that the entire volume of the dunes is composed of mobile sand. The alternative, a mobile rippled skin over an indurated sand core, cannot be maintained for long time periods and is therefore improbable. The measured ripple reptation flux implies a rapid erosion rate of $\sim$0.01 $\mathrm{m\,yr^{-1}}$ (mean dune speed of 0.1 $\mathrm{m\,yr^{-1}}$, multiplied by the tangent of the average stoss slope (6°)). In the absence of a net influx from saltation to compensate for this erosion, the dunes would erode very rapidly. Because saltation drives reptation, the two processes scale[17,18], so that saltation flux should increase up the stoss slope in proportion to the reptation flux. This implies dune erosion as great as 0.05 $\mathrm{m\,yr^{-1}}$. Such a rapid rate would quickly erode any mobile sand layer and expose the indurated core, effectively shutting off subsequent ripple migration. In this picture, the Nili ripple migration rates and patterns would represent a very short time window (maximum duration of the order of the turnover time—a few hundred to a few thousand years) following the formation of an immobile dune core. Finding the dunes in this rare state seems very improbable. More likely is that erosion of the stoss slope is compensated by deposition on the lee front, resulting in whole dune migration and complete recycling of the entire dune volume.

These results demonstrate that conditions in Nili Patera, and probably over much of Mars, are sufficient to move large dunes and transport fluxes of sand equivalent to those on Earth. This is in contrast to predictions from the Ames General Circulation Model (GCM)[2] that threshold wind speeds sufficient to move sand at Nili Patera should not occur. The spatial resolution of GCMs is insufficient to resolve boundary-layer turbulence that may cause gusts above threshold[20]. Even mesoscale simulations need a spatial resolution of kilometres to a few hundred metres to properly model the atmospheric turbulence that accounts for topography and thermal contrasts at the scales of individual dunes[21,22]. The work exemplified in this study can be applied to other regions of Mars, thereby providing ground calibrations for GCMs and mesoscale models, and descriptions of small-scale atmospheric turbulence.

The occurrence of such large sand fluxes, despite the limited winds in Mars' low-density atmosphere[1,2], is probably related to fundamental differences in how sand is mobilized by the wind on Mars compared to

Earth. Although saltation due to aerodynamic shear at fluid threshold is required to initiate grain motion, once started, the sand ejection resulting from grain impact is the major contributor to the particle flux. On Earth, this results in the wind speed required to maintain saltation being about 80% that required for initiation[23]. But because of the higher and longer saltation trajectories on Mars, grains are accelerated to a greater fraction of the wind speed than on Earth, resulting in impact threshold speeds that are only about 10% of the fluid threshold, equivalent in magnitude to that on Earth[24]. Thus, once saltation is initiated by low-frequency gusts, moderate wind speeds can maintain significant fluxes of sand.

To assess the derived sand fluxes in regard to landscape modification, we consider the abrasion susceptibility, S_a, defined as the mass of sand required to erode a unit mass of rock. For basalt grains striking basaltic rocks at the impact threshold for Mars, $S_a = 2 \times 10^{-6}$ (ref. 25). The average flux of $2.3\,\mathrm{m^3\,m^{-1}\,yr^{-1}}$ implies that for the saltation trajectories of 0.1–0.5 m that are likely on Mars[24], the abrasion rate would be $\sim$1–10 μm yr^{-1} on flat ground, and $\sim$10–50 μm yr^{-1} for a vertical rock face (see Supplementary Information), spanning field measurements of basalt abrasion rates in Victoria Valley of $\sim$30–50 μm yr^{-1} (ref. 26).

One view of Mars has been that conditions since the end of the Hesperian period (1.8–3.5 Gyr ago) have been fairly static, with very low erosion rates[27]. This study shows that this is not the case at Nili Patera, and probably not at other areas of Mars where there are significant gusts of sand and wind. This may explain why vast areas of the Martian surface show evidence of erosion and removal, including of mantle materials for which the processes and agents of exhumation have been a mystery[7], yet also contain fields of large dunes that migrate at relatively slow rates. Over long time periods, it may be that much or all of Mars has been subjected to large sand fluxes, with associated erosional modification of the landscape. The techniques reported here can be applied to many dunes and other slowly changing features on Mars and Earth, allowing sand flux and landscape modification to be assessed in a variety of terrains, latitudes, seasons and climates.

Received 6 September 2011; accepted 6 March 2012.
Published online 9 May 2012.

1. Arvidson, R. E., Guinness, E. A., Moore, H. J., Tillman, J. & Wall, S. D. Three Mars years: Viking Lander 1 imaging observations. *Science* **222,** 463–468 (1983).
2. Haberle, R. M., Murphy, J. R. & Schaeffer, J. Orbital change experiments with a Mars General Circulation Model. *Icarus* **161,** 66–89 (2003).
3. Silvestro, S., Fenton, L. K., Vaz, D. A., Bridges, N. T. & Ori, G. G. Ripple migration and dune activity on Mars: Evidence for dynamic processes. *Geophys. Res. Lett.* **37,** L20203 (2010).
4. Chojnacki, M., Burr, D. M., Moersch, J. E. & Michaels, T. I. Orbital observations of contemporary dune activity in Endeavour Crater, Meridiani Planum, Mars. *J. Geophys. Res.* **116,** E00F19 (2011).
5. Hansen, C. J. *et al.* Seasonal erosion and restoration of Mars' northern polar dunes. *Science* **331,** 575–578 (2011).
6. Bridges, N. T. *et al.* Planet-wide sand motion on Mars. *Geology* **40,** 31–34 (2012).
7. Malin, M. C. & Edgett, K. S. Mars Global Surveyor Mars Orbiter Camera: Interplanetary cruise through primary mission. *J. Geophys. Res.* **106,** 23,429–23,570 (2001).
8. Laity, J. E. & Bridges, N. T. Ventifacts on Earth and Mars: Analytical, field, and laboratory studies supporting sand abrasion and windward feature development. *Geomorphology* **105,** 202–217 (2009).
9. Claudin, P. & Andreotti, B. A scaling law for aeolian dunes on Mars, Venus, Earth, and for subaqueous ripples. *Earth Planet. Sci. Lett.* **252,** 30–44 (2006).
10. Sullivan, R. *et al.* Wind-driven particle mobility on Mars: Insights from Mars Exploration Rover observations at "El Dorado" and surroundings at Gusev Crater. *J. Geophys. Res.* **113,** E06S07 (2008).
11. Armstrong, J. C. & Leovy, C. B. Long-term wind erosion on Mars. *Icarus* **176,** 57–74 (2005).
12. Leprince, S., Barbot, S., Ayoub, F. & Avouac, J. P. Automatic and precise orthorectification, coregistration, and subpixel correlation of satellite images, application to ground deformation measurements. *IEEE Trans. Geosci. Rem. Sens.* **45,** 1529–1558 (2007).
13. Vermeesch, P. & Drake, N. Remotely sensed dune celerity and sand flux measurements of the world's fastest barchans (Bodélé, Chad). *Geophys. Res. Lett.* **35,** L24404 (2008).
14. McEwen, A. S. *et al.* The High Resolution Imaging Science Experiment (HiRISE) during MRO's Primary Science Phase (PSP). *Icarus* **205,** 2–37 (2010).
15. Ould Ahmedou, D. *et al.* Barchan dune mobility in Mauritania related to dune and interdune sand fluxes. *J. Geophys. Res.* **112,** F02016 (2007).
16. Andreotti, B., Claudin, P. & Pouliquen, O. Aeolian sand ripples: experimental evidence of fully developed states. *Phys. Rev. Lett.* **96,** 028001 (2006).
17. Anderson, R. S. A theoretical model for aeolian impact ripples. *Sedimentology* **34,** 943–956 (1987).
18. Andreotti, B. A two-species model of aeolian sand transport. *J. Fluid Mech.* **510,** 47–70 (2004).
19. Bourke, M. C., Ewing, R. C., Finnegan, D. & McGowan, H. A. Sand dune movement in Victoria Valley, Antarctica. *Geomorphology* **109,** 148–160 (2009).
20. Fenton, L. K. & M. i. c. h. a. e. l. s. T. J. Characterizing the sensitivity of daytime turbulent activity on Mars with the MRAMS LES: early results. *Mars* **5,** 159–171 (2010).
21. Fenton, L. J., Toigo, A. & Richardson, M. I. Aeolian processes in Proctor Crater on Mars: mesoscale modeling of dune-forming winds. *J. Geophys. Res.* **110,** E06005 (2005).
22. Spiga, A. & Forget, F. A new model to simulate the Martian mesoscale and microscale atmospheric circulation: validation and first results. *J. Geophys. Res.* **114,** E02009 (2009).
23. Bagnold, R. A. *The Physics of Blown Sand and Desert Dunes* (Dover Publications, 1954).
24. Kok, J. F. Difference in the wind speeds required for initiation versus continuation of sand transport on Mars: implications for dunes and dust storms. *Phys. Rev. Lett.* **104,** 074502 (2010).
25. Greeley, R. *et al.* Rate of wind abrasion on Mars. *J. Geophys. Res.* **87,** 10,009–10,024 (1982).
26. Malin, M. C. Rates of geomorphic modification in ice-free areas, southern Victoria Land, Antarctica. *Antarct. J. US* **20,** 18–21 (1986).
27. Golombek, M. P. *et al.* Erosion rates at the Mars Exploration Rover landing sites and long-term climate change on Mars. *J. Geophys. Res.* **111,** E12S10 (2006).
28. Long, J. T. & Sharp, R. S. Barchan-dune movement in Imperial Valley, California. *Geol. Soc. Am. Bull.* **75,** 149–156 (1964).
29. Fryberger, S. *et al.* Wind sedimentation in the Jafurah sand sea, Saudi Arabia. *Sedimentology* **31,** 413–431 (1984).
30. Lancaster, N. Controls on aeolian activity: some new perspectives from the Kelso Dunes, Mojave Desert, California. *J. Arid Environ.* **27,** 113–125 (1994).

Supplementary Information is linked to the online version of the paper at www.nature.com/nature.

Acknowledgements Discussions with R. Ewing, C. Narteau, and S. Silvestro on bedforms and R. Kirk on stereo data significantly improved this research. This research was supported by grants from NASA's Mars Data Analysis Program, the Keck Institute for Space Studies, and seed funding from the Jet Propulsion Laboratory's Director's Research and Development Fund.

Author Contributions N.T.B. is the principal investigator of the NASA MDAP grant that partially funded this work, chose the study area, defined major science questions, participated in data analysis, compared results to other Mars and terrestrial data, and led the writing of the paper. F.A. processed all the data with COSI-Corr, produced the figures and Supplementary Information ancillary materials, and played a major role in quantitative analysis and text writing. J-P.A. initiated the project, contributed fundamental ideas on sand flux and dune movement, supervised the data analysis and contributed to text writing. S.L. evaluated all COSI-Corr and quantitative results. A.L. provided expertise in interpretation of bedform movement and sand flux in regards to Mars surface evolution and climate models. S. M. produced the digital elevation model. All authors shared ideas and results and helped produce the final manuscript.

Author Information Reprints and permissions information is available at www.nature.com/reprints. The authors declare no competing financial interests. Readers are welcome to comment on the online version of this article at www.nature.com/nature. Correspondence and requests for materials should be addressed to N.T.B. (nathan.bridges@jhuapl.edu).